J. Fluid Mech. (2009), *vol.* 641, *pp.* 475–487.
doi:10.1017/S0022112009992163

Three-dimensional absolute and convective instabilities at the onset of convection in a porous medium with inclined temperature gradient and vertical throughflow

LEONID BREVDO†

Institute of Fluid and Solid Mechanics, University of Strasbourg/CNRS, 2 rue Boussingault, F 67000 Strasbourg, France

(Received 14 April 2009; revised 9 September 2009; accepted 9 September 2009; first published online 25 November 2009)

By using the mathematical formalism of absolute and convective instabilities, we study in this work the nature of unstable three-dimensional localized disturbances at the onset of convection in a flow in a saturated homogeneous porous medium with inclined temperature gradient and vertical throughflow. It is shown that for marginally supercritical values of the vertical Rayleigh number R_v the destabilization has the character of absolute instability in all the cases in which the horizontal Rayleigh number R_h is zero or the Péclet number Q_v is zero. In all the cases in which R_h and Q_v are both different from zero, at the onset of convection the instability is convective. In the latter cases, the growing emerging disturbance has locally the structure of a non-oscillatory longitudinal roll, and its group velocity points in the direction opposite the direction of the applied horizontal temperature gradient, i.e. parallel to the axis of the roll. The speed of propagation of the unstable wavepacket increases with Q_v and generally increases with R_h.

Key words: absolute/convective, porous media

1. Introduction

The question of the onset of convection in a porous medium with inclined temperature gradient has received considerable attention in the literature owing to the numerous environmental, geophysical and industrial applications (for detailed reviews, see Bear 1988; Nield & Bejan 2006; Straughan 2004*b*). Since the publication of the seminal work of Weber (1974) a large number of papers were published that dealt with the natural and forced convection in a horizontal porous layer with inclined temperature gradient. In many studies of convection in a porous medium, the medium is modelled as an extended horizontal saturated porous layer in which the flow motion is induced by either the horizontal or the vertical or inclined temperature and/or salinity gradients, including the Soret effect (see for example Nield 1991, 1994; Nield, Manole & Lage 1993; Straughan & Walker 1996; Bahloul, Boutana & Vasseur 2003; Straughan 2004*a*; Delache, Ouarzazi & Combarnous 2007; Delache & Ouarzazi 2008; Narayana, Murthy & Gorla 2008; Ouarzazi *et al.* 2008 and the references therein). The extended-layer model is employed to facilitate the analysis and, in particular, to make possible the application of analytic treatments such as

† Email address for correspondence: Leonid.Brevdo@imfs.u-strasbg.fr

the treatment of a single monochromatic wave and the stability treatment by using a Fourier transform in space. The model is used based on the assumption that the emergence and evolution of convection rolls of finite diameter in a porous layer of finite horizontal extent can be well modelled in an extended layer provided that the finite horizontal extent of the porous layer is much greater than the diameter of the convection rolls.

It was shown by Nield (1990) and Qiao & Kaloni (1997) that a mean horizontal mass flow superimposed on a Hadley circulation, driven by the horizontal component of an inclined thermal gradient, influences considerably the flow dynamics in a porous layer. The circulation is named after George Hadley, an English meteorologist of the 18th century, who first described an atmospheric flow induced by the horizontal component of an inclined temperature gradient in his study of the cause of the trade winds (see Persson 2006 for a description). Since the Hadley circulation in the central portion of the flow is approximately independent of horizontal position, in this portion it can be modelled as a uniform flow. The influence on the onset of convection of a vertical mass flow superimposed on a Hadley circulation in a model of a horizontal porous layer with inclined temperature gradient was first studied by Nield (1998). In that work, it was reported that the vertical mass flow renders the model less unstable and, at the onset of instability, renders the diameter of the convection rolls smaller.

Until recently, in the analyses of the onset of convection in an extended horizontal layer of a porous medium only the sinusoidal disturbances, i.e. normal modes, were treated. A treatment of normal modes is indispensable in any stability analysis of an extended medium because it first and foremost provides one with the critical values of the corresponding control parameter. However, in order to obtain an information concerning the evolution of localized perturbations one has to resort to a different tool, specifically to a treatment of an initial-value problem formulated for the linearized equations of motion and to an analysis of absolute and convective instabilities.

The theory of two-dimensional absolute and convective instabilities of extended homogeneous flows has its origin in the physics literature, with the main ideas being put forward as early as in 1949 by Landau and Lifshitz (see e.g. Landau & Lifshitz 1959). Since the early 1950s, starting with the work of Twiss (1951), the evolution of two-dimensional linear wavepackets in spatially homogeneous extended flows was an area of active interest in the plasma physics literature. The modern mathematical foundations of the formalism of two-dimensional absolute and convective instabilities of uniform flows were laid down by Briggs (1964). In fluid mechanics, the dynamics of unstable linear wavepackets in homogeneous open flows have attracted considerable attention since the early 1960s because of the significance of localized waves in the transition to turbulence (see Gaster 1968, 1975; Gaster & Grant 1975; Drazin & Reid 1981 and the references therein).

In a recent work, Brevdo & Ruderman (2009*a*,*b*) applied the formalism of absolute and convective instabilities for studying the onset of convection in the model of a two-dimensional flow in a horizontal extended porous layer with inclined temperature gradient and vertical throughflow that was previously treated on stability of normal modes by Nield (1998). In the work of Brevdo & Ruderman (2009*a*,*b*), the stability results of Nield (1998) were confirmed including the conjecture that among the two-dimensional modes the longitudinal mode is favourable for the onset of convection and that all the longitudinal modes are non-oscillatory, for all the values of the parameters considered. This implies that in the two-dimensional approach, the onset of convection occurs through absolute instability. Further, Brevdo & Ruderman

(2009*a*,*b*) treated transverse perturbations and discovered an absolute–convective instability dichotomy in a set of exact solutions of the equations of motion at the point of destabilization of such perturbations. The dependence of the dichotomy on the horizontal Rayleigh number R_h and on the Péclet number Q_v was investigated.

In the present paper, we address the nature of instability of three-dimensional wavepackets in the model at the onset of convection by using the extension made by Brevdo (1991) of the Briggs formalism of two-dimensional absolute and convective instabilities to the three-dimensional case. We show that among the three-dimensional normal modes, the longitudinal mode is still favourable and that, consequently, at the onset of convection unstable three-dimensional wavepackets have the local structure of a non-oscillatory longitudinal roll. However, in contrast with the two-dimensional case, such wavepackets are absolutely unstable only in the cases in which $R_h = 0$ or $Q_v = 0$. When both R_h and Q_v are different from zero, the instability at the onset of convection is convective.

The paper is organized as follows. In § 2, we describe the model, give the governing equations and present the base solution. Section 3 describes a linear initial-value problem and a Laplace–Fourier-transformed problem and gives an expression for the solution of the initial-value problem. In § 4, a procedure for analysing a marginally unstable state on three-dimensional absolute and convective instabilities is described, and a numerical treatment of the homogeneous boundary-value problem is outlined. In § 5, the stability results are presented, and in § 6 conclusions are made.

2. Formulation

In our description of the model, we adopt the assumptions, notations and non-dimensionalization of Nield (1998).

We treat a three-dimensional flow in a homogeneous saturated porous medium that occupies an extended horizontal layer of height H. The origin of the Cartesian coordinates is placed at the mid-height of the layer, with the z^*-axis pointing vertically upwards and the x^*-axis pointing in the direction opposite the direction of the applied horizontal temperature gradient β. Here and further in the text, the superscript '*' denotes dimensional quantities. The vertical temperature difference across the boundaries is ΔT, and the vertical throughflow velocity is denoted by w_v. The flow in the porous medium is assumed to be governed by the Darcy law, and the Oberbeck–Boussinesq approximation applies (see Bear 1988). The horizontal net flow is supposed to be zero.

The governing equations for the flow read

$$\left.\begin{gathered} \nabla^* \cdot \boldsymbol{v}^* = 0, \\ \nabla^* P^* + \frac{\mu}{K}\boldsymbol{v}^* - \rho_f^* \boldsymbol{g} = 0, \\ (\rho c)_m \frac{\partial T^*}{\partial t^*} + (\rho c_p)_f \boldsymbol{v}^* \cdot \nabla^* T^* = k_m \nabla^{*2} T^*, \\ \rho_f^* = \rho_0[1 - \gamma(T^* - T_0)], \\ -\infty < x^*, y^* < \infty, \quad -H/2 < z^* < H/2, \quad t^* > 0, \end{gathered}\right\} \tag{2.1}$$

where ∇ is the gradient operator; $\boldsymbol{v}^* = (u^*, v^*, w^*)^T$, t^*, P^* and T^* denote the Darcy velocity, time, pressure and temperature, respectively; the subscripts m, f and 0 refer to the porous medium, the fluid and the uniform reference state, respectively; $\boldsymbol{g} = (0, 0, -g)^T$ is the gravity acceleration vector; μ, ρ and c are viscosity, density

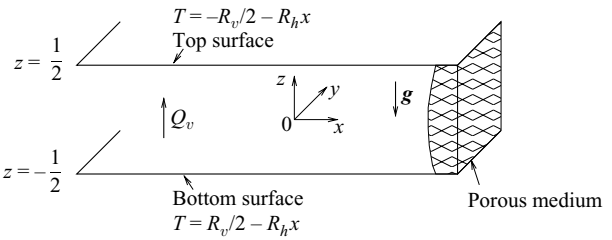

FIGURE 1. Sketch of the model of a flow in a horizontal porous layer with scaled notations.

and specific heat, respectively; K is the permeability of the porous medium; k_m is the effective thermal conductivity of the porous matrix; and γ denotes the thermal expansion coefficient of the fluid. The boundary conditions are

$$w^* = w_v, \quad T^* = T_0 \mp \Delta T/2 - \beta x^* \quad \text{at} \quad z^* = \pm H/2. \tag{2.2}$$

Non-dimensionalized quantities are defined by

$$\left.\begin{aligned} (x, y, z) = (x^*, y^*, z^*)/H, \quad t = \alpha_m t^*/(AH^2), \quad \boldsymbol{v} = \boldsymbol{v}^* H/\alpha_m, \\ P = K(P^* + \rho_0 g z^*)/(\mu\alpha_m), \quad T = (T^* - T_0)\frac{\rho_0 g \gamma K H}{\mu\alpha_m}, \end{aligned}\right\} \tag{2.3}$$

where $\alpha_m = k_m/(\rho c_p)_f$ and $A = (\rho c)_m/(\rho c_p)_f$. The non-dimensionalized governing equations now read

$$\left.\begin{aligned} \nabla \cdot \boldsymbol{v} = 0, \\ \nabla P + \boldsymbol{v} - T\boldsymbol{k} = 0, \\ \frac{\partial T}{\partial t} + \boldsymbol{v} \cdot \nabla T = \nabla^2 T, \\ -\infty < x, y < \infty, \quad -1/2 < z < 1/2, \quad t > 0, \end{aligned}\right\} \tag{2.4}$$

and the scaled boundary conditions are

$$w = Q_v, \quad T = \mp R_v/2 - R_h x \quad \text{at} \quad z = \pm 1/2, \tag{2.5}$$

where $\boldsymbol{k} = (0, 0, 1)^T$, and the non-dimensional parameters in (2.5) are the vertical Rayleigh number (R_v), the horizontal Rayleigh number (R_h) and the Péclet number (Q_v) given by a definition sketch of the model in non-dimensionalized notations is shown in figure 1.

$$R_v = \frac{\rho_0 g \gamma K H \Delta T}{\mu\alpha_m}, \quad R_h = \frac{\rho_0 g \gamma K H^2 \beta}{\mu\alpha_m} \quad \text{and} \quad Q_v = \frac{w_v H}{\alpha_m}. \tag{2.6}$$

Problem (2.4)–(2.5) possesses a stationary flow solution with zero horizontal net flow. The solution is given by

$$\left.\begin{aligned} U_s = R_h z, \quad W_s = Q_v, \quad V_s = 0, \\ T_s = \frac{R_h^2}{2Q_v}\left(z^2 - \frac{1}{4}\right) + \frac{R_h^2}{Q_v^2} z - \frac{Q_v^2 R_v + R_h^2}{2Q_v^2 \sinh(Q_v/2)}\left[\mathrm{e}^{Q_v z} - \cosh(Q_v/2)\right] - R_h x \end{aligned}\right\} \tag{2.7}$$

(see Nield 1998).

3. Initial- and boundary-value problems

We linearize the equations of motion (2.4) around solution (2.7) and by assuming the presence of momentum and energy sources and perturbations at the upper and lower boundaries of the layer write an initial-value problem for the linearized equations as

$$\left.\begin{gathered}\frac{\partial u'}{\partial x}+\frac{\partial v'}{\partial y}+\frac{\partial w'}{\partial z}=0,\\ \frac{\partial p'}{\partial x}+u'=m_x,\quad \frac{\partial p'}{\partial y}+v'=m_y,\quad \frac{\partial p'}{\partial z}+w'-\theta'=m_z,\\ \frac{\partial \theta'}{\partial t}+U_s\frac{\partial \theta'}{\partial x}+Q_v\frac{\partial \theta'}{\partial z}-R_h u'+\frac{\mathrm{d}T_s}{\mathrm{d}z}w'-\frac{\partial^2\theta'}{\partial x^2}-\frac{\partial^2\theta'}{\partial y^2}-\frac{\partial^2\theta'}{\partial z^2}=e,\\ -1/2<z<1/2,\quad -\infty<x,y<\infty,\quad t>0,\\ (\boldsymbol{v}',p',\theta')|_{t=0}=(\boldsymbol{v}_0,p_0,\theta_0)(z,x,y),\\ (\boldsymbol{v}',p',\theta')\big|_{z=-1/2}=(\boldsymbol{v}_1,p_1,\theta_1)(x,y,t),\quad (\boldsymbol{v}',p',\theta')\big|_{z=1/2}=(\boldsymbol{v}_2,p_2,\theta_2)(x,y,t).\end{gathered}\right\}\tag{3.1}$$

Here, the prime denotes perturbation quantities. Further in the text the prime will be dropped for convenience. The functions $m_x=m_x(z,x,y,t)$, $m_y=m_y(z,x,y,t)$, $m_z=m_z(z,x,y,t)$, $e=e(z,x,y,t)$, $\boldsymbol{v}_{1,2}(x,y,t)$, $p_{1,2}(x,y,t)$ and $\theta_{1,2}(x,y,t)$ are supposed to have finite support in x, y and t, and the functions $\boldsymbol{v}_0(z,x,y)$, $p_0(z,x,y)$ and $\theta_0(z,x,y)$ are supposed to have finite support in x and y.

Elimination of u, v, p and θ from the equations in (3.1) in a way similar to that used by Brevdo & Ruderman (2009*b*) in the treatment of the two-dimensional case results in an equation for the vertical perturbation velocity w,

$$\left.\begin{gathered}\left[\left(\frac{\partial}{\partial t}+U_s\frac{\partial}{\partial x}+Q_v\frac{\partial}{\partial z}-\frac{\partial^2}{\partial x^2}-\frac{\partial^2}{\partial y^2}-\frac{\partial^2}{\partial z^2}\right)\left(\frac{\partial^2}{\partial x^2}+\frac{\partial^2}{\partial y^2}+\frac{\partial^2}{\partial z^2}\right)\right.\\ \left.+R_h\frac{\partial^2}{\partial x\partial z}+\frac{\mathrm{d}T_s}{\mathrm{d}z}\left(\frac{\partial^2}{\partial x^2}+\frac{\partial^2}{\partial y^2}\right)\right]w(z,x,y,t)=E(z,x,y,t),\\ -1/2<z<1/2,\quad -\infty<x,y<\infty,\quad t>0,\end{gathered}\right\}\tag{3.2}$$

where $E(z,x,y,t)$ being a linear combination of the source functions and their derivatives is a function with finite support in x, y and t. The initial and boundary conditions for w are

$$\left.\begin{gathered}w|_{t=0}=w_0(z,x,y),\\ w=f_1(x,y,t),\quad \frac{\partial^2 w}{\partial z^2}=f_3(x,y,t)\quad \text{at}\quad z=-1/2,\\ w=f_2(x,y,t),\quad \frac{\partial^2 w}{\partial z^2}=f_4(x,y,t)\quad \text{at}\quad z=1/2.\end{gathered}\right\}\tag{3.3}$$

The boundary conditions are derived from the equations and boundary conditions in (3.1) (cf. Brevdo & Ruderman 2009*b*).

We operate on problem (3.2)–(3.3) with the Laplace transform in time and the double Fourier transform in x and y defined as

$$L\{w\}(\omega)=\widetilde{w}(\omega)=\int_0^\infty w(t)\mathrm{e}^{\mathrm{i}\omega t}\mathrm{d}t,\quad w(t)=\frac{1}{2\pi}\int_{\mathrm{i}\sigma-\infty}^{\mathrm{i}\sigma+\infty}\widetilde{w}(\omega)\mathrm{e}^{-\mathrm{i}\omega t}\mathrm{d}\omega\tag{3.4}$$

and

$$\left.\begin{aligned} F\{u\}(k,l) = \widehat{u}(k,l) &= \int_{-\infty}^{\infty}\int_{-\infty}^{\infty} u(x,y)\mathrm{e}^{-\mathrm{i}(kx+ly)}\,\mathrm{d}x\,\mathrm{d}y, \\ u(x,y) &= \frac{1}{4\pi^2}\int_{-\infty}^{\infty}\int_{-\infty}^{\infty} \widehat{u}(k,l)\mathrm{e}^{\mathrm{i}(kx+ly)}\,\mathrm{d}k\,\mathrm{d}l, \end{aligned}\right\} \tag{3.5}$$

respectively. As a result we obtain the boundary-value problem for the transformed function $w(z,k,l,\omega)$:

$$\left.\begin{aligned} &\left[\left(\frac{\mathrm{d}^2}{\mathrm{d}z^2} - k^2 - l^2 + \mathrm{i}\omega - \mathrm{i}kU_s - Q_v\frac{\mathrm{d}}{\mathrm{d}z}\right)\left(\frac{\mathrm{d}^2}{\mathrm{d}z^2} - k^2 - l^2\right)\right. \\ &\quad \left. - \mathrm{i}kR_h\frac{\mathrm{d}}{\mathrm{d}z} + (k^2+l^2)\frac{\mathrm{d}T_s}{\mathrm{d}z}\right] w(z,k,l,\omega) = S(z,k,l,\omega), \quad -1/2 < z < 1/2, \\ &w = f_1(k,l,\omega), \quad \frac{\mathrm{d}^2 w}{\mathrm{d}z^2} = f_3(k,l,\omega) \quad \text{at} \quad z = -1/2, \\ &w = f_2(k,l,\omega), \quad \frac{\mathrm{d}^2 w}{\mathrm{d}z^2} = f_4(k,l,\omega) \quad \text{at} \quad z = 1/2. \end{aligned}\right\} \tag{3.6}$$

In (3.6) and further in the text the tilde and the hat are omitted for convenience. We distinguish dependent variables from their transforms by the independent variables. The function $S(z,k,l,\omega)$ in (3.6) is a linear combination of the transformed initial and boundary conditions and their transformed derivatives.

Problem (3.6) is similar to problem (9) in Brevdo & Ruderman (2009*b*); its solution is also similar to the solution of problem (9) of the same work. To avoid repetition we omit the details of the solution and present here the final results. The solution of problem (3.6) is given by

$$w(z,k,l,\omega) = \frac{T(z,k,l,\omega)}{\mathrm{e}^{Q_v z}D(k,l,\omega)}, \tag{3.7}$$

where $T(z,k,l,\omega)$ depends linearly on the functions $S(z,k,l,\omega)$ and $f_i(k,l,\omega)$, $1 \leqslant i \leqslant 4$, and $D(k,l,\omega)$ is the dispersion-relation function of the problem. The construction of $T(z,k,l,\omega)$ and $D(k,l,\omega)$ can be made in a fashion similar to that used by Brevdo & Ruderman (2009*b*) to construct the corresponding functions $T(z,k,\omega)$ and $D(k,\omega)$, in the two-dimensional case. A triple (k,l,ω) satisfies the dispersion relation,

$$D(k,l,\omega) = 0, \tag{3.8}$$

if and only if there exists a non-trivial solution of the homogeneous boundary-value problem associated with problem (3.6):

$$\left.\begin{aligned} &\left[\left(\frac{\mathrm{d}^2}{\mathrm{d}z^2} - k^2 - l^2 + \mathrm{i}\omega - \mathrm{i}kU_s - Q_v\frac{\mathrm{d}}{\mathrm{d}z}\right)\left(\frac{\mathrm{d}^2}{\mathrm{d}z^2} - k^2 - l^2\right)\right. \\ &\quad \left. - \mathrm{i}kR_h\frac{\mathrm{d}}{\mathrm{d}z} + (k^2+l^2)\frac{\mathrm{d}T_s}{\mathrm{d}z}\right] w(z,k,l,\omega) = 0, \quad -1/2 < z < 1/2, \\ &w = 0, \quad \frac{\mathrm{d}^2 w}{\mathrm{d}z^2} = 0 \quad \text{at} \quad z = \pm 1/2. \end{aligned}\right\} \tag{3.9}$$

The solution of the initial-value problem (3.2)–(3.3) is formally expressed by

$$w(z,x,y,t) = \frac{1}{8\pi^3\mathrm{e}^{Q_v z}}\int_{\mathrm{i}\sigma-\infty}^{\mathrm{i}\sigma+\infty}\int_{-\infty}^{\infty}\int_{-\infty}^{\infty}\frac{T(z,k,l,\omega)}{D(k,l,\omega)}\,\mathrm{e}^{\mathrm{i}(kx+ly-\omega t)}\,\mathrm{d}k\,\mathrm{d}l\,\mathrm{d}\omega. \tag{3.10}$$

Here σ is a real number that is greater than the maximum growth rate of the normal modes, i.e.

$$\sigma > \sigma_m = \max\{\mathrm{Im}\ \omega \mid D(k, l, \omega) = 0,\ \mathrm{Im}\ k = 0, \mathrm{Im}\ l = 0\}. \tag{3.11}$$

4. Treatment of absolute and convective instabilities

A formalism for treating three-dimensional absolute and convective instabilities in a homogeneous state was developed by Brevdo (1991) by using the approach developed by Briggs (1964) for the analysis of two-dimensional instabilities. Determining the points that contribute to the instabilities in the three-dimensional case generally requires solving a system of three equations of the form $D = 0$, $\partial D/\partial k + U\,\partial D/\partial\omega = 0$, $\partial D/\partial l + V\,\partial D/\partial\omega = 0$, in the three-dimensional complex space of (k, l, ω). Computationally, this might be a rather involved task, unless $D(k, l, \omega)$ is given explicitly and has a simple form.

In the present case, however, we are interested only in the nature of instability at the onset of convection, that is to say at a marginally supercritical value of the control parameter. The control parameter in our treatment is the vertical Rayleigh number, R_v. For analysing the nature of destabilization, it is sufficient to compute the group velocity vector (V_{gx}, V_{gy}) of the unstable wavepacket of a marginally unstable state. The components of this vector are computed as

$$V_{gx} = \frac{\partial\omega_r(k_c, l_c)}{\partial k} \quad \text{and} \quad V_{gy} = \frac{\partial\omega_r(k_c, l_c)}{\partial l}, \tag{4.1}$$

where (k_c, l_c) is the critical wavenumber vector (cf. Brevdo 1991). Here and further in the text, the subscript r denotes the real part and the subscript i denotes the imaginary part of a complex number. When $(V_{gx}, V_{gy}) = (0, 0)$ the base state is absolutely unstable. In the case in which $(V_{gx}, V_{gy}) \neq 0$ and $\sqrt{V_{gx}^2 + V_{gy}^2}$ is large enough the flow at the onset of convection is absolutely stable but convectively unstable. This is so because, owing to continuity, the group velocity vector varies only slightly when the marginally supercritical vertical Rayleigh number, R_v, is brought down towards its critical value R_{vc}, whereas the set of unstable velocity vectors shrinks and eventually reduces to the group velocity vector, which remains different from zero, as R_v reaches R_{vc}. Our computations confirmed this assertion in all the cases considered.

For analysing the instabilities, we computed numerically the frequency, ω, as a function of real k and l by discretizing problem (3.9) and finding all the eigenvalues in ω of the resulting generalized algebraic eigenvalue problem. For the discretization, a Chebyshev collocation method was used. The algebraic eigenvalue problem was solved using the global solver DGVLCG of the International Mathematical and Statistical Library. The procedure is described in detail by Brevdo & Ruderman (2009*a*).

5. Stability results

To illustrate the three-dimensional stability computations, we present in figures 2–4 the graphs of the surfaces $\omega_i = \omega_i(k, l)$ and $\omega_r = \omega_r(k, l)$ and the contour lines of the surface of $\omega_i = \omega_i(k, l)$, respectively, for the marginally unstable mode, for the case $R_h = 30$, $Q_v = 4$. The results are shown in the first quadrant of the real (k, l)-plane. The graphs in the whole real (k, l)-plane are obtained by symmetry, as $\omega_i = \omega_i(k, l)$ is an even function of real k and l, and $\omega_r = \omega_r(k, l)$ is an odd function of real k and

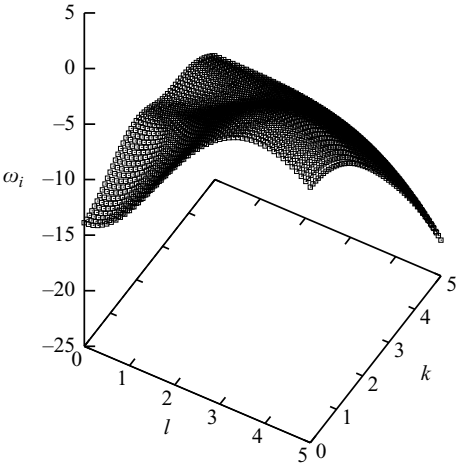

FIGURE 2. Growth rate ω_i of the marginally unstable mode as a function of real k and l, for $R_h = 30,\ Q_v = 4$. The marginally supercritical vertical Rayleigh number is $R_{vc} = 83.786$.

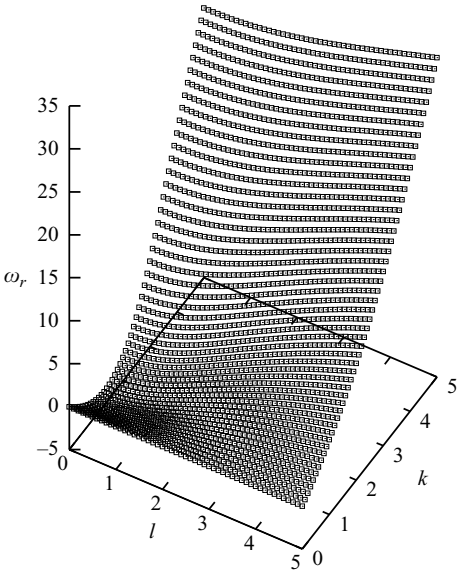

FIGURE 3. Real part of the frequency ω_r of the marginally unstable mode as a function of real k and l. The parameters are as in figure 2.

an even function of real l. This can be seen by considering the complex conjugate of problem (3.9).

In three tables, we present the computation results for various values of R_h and Q_v. In table 1, slightly supercritical values of the vertical Rayleigh number, R_{vc}, are given. In each case, the flow is unstable for the value of R_{vc} shown in that table, and it is stable for the value of R_v obtained from R_{vc} by reducing by 1 the last significant digit in the number giving R_{vc}. Thus, in the $R_h = 30,\ Q_v = 4$ case illustrated in figures 2–4 the base state is unstable for $R_v = 83.786$, and it is stable for $R_v = 83.785$. The results given in tables 2 and 3 are computed to the accuracy of one half of the decimal position, 0.5×10^{-p}, that follows the last decimal position shown in each number.

	$R_h = 0$	10	20	30	40	50	60
$Q_v = 0$	39.479	42.008	49.549	61.957	78.967	100.12	124.48
1	40.876	43.404	50.941	63.336	80.317	101.41	125.65
2	45.078	47.604	55.128	67.487	84.381	105.29	129.19
3	52.069	54.589	62.088	74.382	91.128	111.74	135.05
4	61.668	64.172	71.617	83.786	100.28	120.39	142.53
5	73.415	75.880	83.189	95.078	111.03	129.93	148.98
6	86.620	88.994	96.008	107.30	122.09	138.83	155.56
7	100.59	102.81	109.33	119.68	132.93	147.74	162.90
8	114.84	116.86	122.77	132.06	143.85	157.13	171.00

TABLE 1. Values of the marginally supercritical vertical Rayleigh number, R_{vc}.

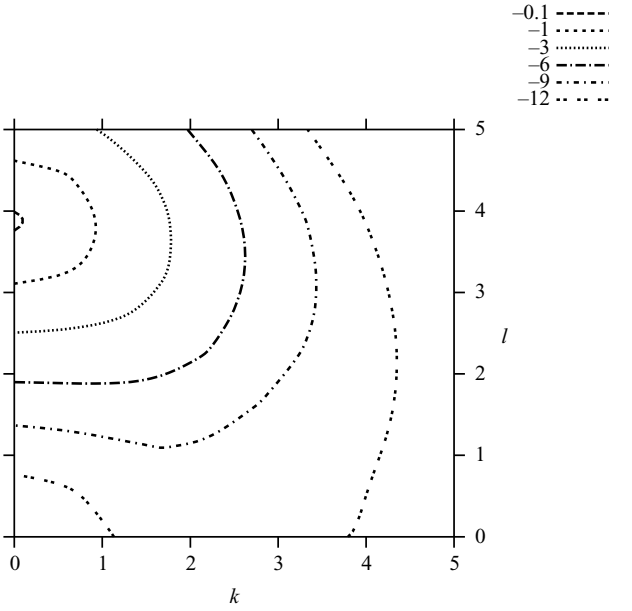

FIGURE 4. Contour lines of $\omega_i = \omega_i(k, l)$ for the marginally unstable mode. The parameters are as in figure 2.

Table 2 shows the values of the critical wavenumber vector (k_c, l_c). The critical wavenumber vector in all the cases has zero k-component, implying that among the three-dimensional normal modes the longitudinal two-dimensional mode is favourable. An illustration of the finding that in the (k, l)-space incipient instability occurs on the l-axis is presented in figure 4. In this figure, six contour lines of the surface $\omega_i = \omega_i(k, l)$ whose graph is shown in figure 2 are plotted, and it is seen that the function $\omega_i = \omega_i(k, l)$ attains its maximum, which in this case is marginally greater than zero, on the l-axis, at $l_c = 3.85$.

The real frequency of the critical mode is zero, in all the cases treated. This is illustrated in figure 3, where it is seen that $\omega_r(0, l) = 0$, for all l. Computations of the critical values of the vertical Rayleigh number and of normal modes in the two-dimensional case were reported by Nield (1998), for the cases considered in the present paper, with an exception of the cases $R_h = 50, 60$. Our results for R_{vc} and k_c

	$R_h=0$	10	20	30	40	50	60
$Q_v=0$	(0, 3.14)	(0, 3.14)	(0, 3.15)	(0, 3.16)	(0, 3.22)	(0, 3.34)	(0, 3.67)
1	(0, 3.18)	(0, 3.18)	(0, 3.18)	(0, 3.20)	(0, 3.25)	(0, 3.38)	(0, 3.71)
2	(0, 3.29)	(0, 3.29)	(0, 3.30)	(0, 3.31)	(0, 3.37)	(0, 3.50)	(0, 3.83)
3	(0, 3.49)	(0, 3.49)	(0, 3.50)	(0, 3.52)	(0, 3.58)	(0, 3.73)	(0, 4.11)
4	(0, 3.79)	(0, 3.79)	(0, 3.81)	(0, 3.85)	(0, 3.95)	(0, 4.19)	(0, 5.12)
5	(0, 4.20)	(0, 4.21)	(0, 4.25)	(0, 4.35)	(0, 4.58)	(0, 5.22)	(0, 6.68)
6	(0, 4.73)	(0, 4.76)	(0, 4.85)	(0, 5.06)	(0, 5.52)	(0, 6.40)	(0, 7.46)
7	(0, 5.38)	(0, 5.42)	(0, 5.58)	(0, 5.89)	(0, 6.45)	(0, 7.24)	(0, 8.10)
8	(0, 6.09)	(0, 6.15)	(0, 6.34)	(0, 6.70)	(0, 7.25)	(0, 7.95)	(0, 8.70)

TABLE 2. Values of the critical wavenumber vector, (k_c, l_c).

	$R_h=0$	10	20	30	40	50	60
$Q_v=0$	(0, 0)	(0, 0)	(0, 0)	(0, 0)	(0, 0)	(0, 0)	(0, 0)
1	(0, 0)	(0.0938, 0)	(0.178, 0)	(0.245, 0)	(0.280, 0)	(0.268, 0)	(0.201, 0)
2	(0, 0)	(0.218, 0)	(0.424, 0)	(0.594, 0)	(0.724, 0)	(0.776, 0)	(0.780, 0)
3	(0, 0)	(0.401, 0)	(0.795, 0)	(1.16, 0)	(1.50, 0)	(1.83, 0)	(2.41, 0)
4	(0, 0)	(0.666, 0)	(1.35, 0)	(2.06, 0)	(2.87, 0)	(4.05, 0)	(8.74, 0)
5	(0, 0)	(1.02, 0)	(2.09, 0)	(3.35, 0)	(5.09, 0)	(8.62, 0)	(15.7, 0)
6	(0, 0)	(1.43, 0)	(2.99, 0)	(4.93, 0)	(7.79, 0)	(12.2, 0)	(17.4, 0)
7	(0, 0)	(1.84, 0)	(3.88, 0)	(6.38, 0)	(9.70, 0)	(13.9, 0)	(18.4, 0)
8	(0, 0)	(2.21, 0)	(4.62, 0)	(7.45, 0)	(10.9, 0)	(14.9, 0)	(19.1, 0)

TABLE 3. Values of the group velocity vector of the three-dimensional wavepacket at the onset of convection.

compare well with the results of Nield (1998) and support his assertion that the onset of convection has a non-oscillatory character.

Table 3 shows the values of the group velocity vector, (V_{gx}, V_{gy}), at the onset of convection. From the results of the table it is seen that in the cases in which $R_h=0$ or $Q_v=0$ the destabilization has the character of absolute instability. In all the cases considered when $R_h\neq 0$ and $Q_v\neq 0$, at the onset of convection the instability is convective and the wavepacket moves in the x-direction. Thus, the growing disturbance moving along the most unstable ray, $\{x=x_0+V_{gx}t, y=y_0+V_{gy}t, t\to\infty\}$, has locally the form of a non-oscillatory longitudinal roll that propagates in the positive x-direction which is opposite the direction of the applied horizontal temperature gradient, that is to say in the direction along the axis of the roll. As seen from the results shown in table 2, at the onset of convection, the diameter $d_c=\pi/l_c$ of the cross-section of the roll is generally a decreasing function of R_h and of Q_v. The speed of propagation of the wavepacket increases with Q_v. Also, greater applied horizontal temperature gradient renders the speed of propagation generally greater.

To conclude this section we recall that $\omega_i(k,l)$ is an even function of real k and l and that $\omega_r(k,l)$ is an odd function of real k and an even function of real l. Therefore, at the onset of convection $\omega_i(k,l)$ attains its maximum both at $(0,l_c)$ and at $(0,-l_c)$, where the values of l_c are given in table 2. From the above property of $\omega_r(k,l)$ it follows that the group velocity vector of the marginally unstable wavepacket computed at the contributing point $(0,-l_c)$ is equal to the group velocity vector computed at the contributing point $(0,l_c)$ (see (4.1)). This means that only one

unstable wavepacket moving in the positive x-direction is present at the onset of instability in the convectively unstable cases considered.

6. Conclusions

In this paper, we treated three-dimensional instabilities at the onset of convection in a model of a flow in a porous medium with inclined temperature gradient and vertical throughflow that was studied previously on instability of the two-dimensional longitudinal normal modes by Nield (1998) and on absolute and convective instabilities of the two-dimensional transverse perturbations by Brevdo & Ruderman (2009*a*,*b*). It was found that among the three-dimensional normal modes the longitudinal mode is the favoured one, and all the longitudinal modes are non-oscillatory, extending the two-dimensional results of Nield (1998) to the three-dimensional case.

Our analysis discovered an absolute–convective instability dichotomy at the onset of three-dimensional convection in a set of base states given by exact analytic solutions of the equations of motion in the model. The dichotomy depends on whether the product $R_h Q_v$ is nil or not. When $R_h Q_v = 0$ the destabilization is through absolute instability; otherwise it is through convective instability. The growing wavepacket has at its peak locally the form of a non-oscillatory longitudinal roll that propagates in the direction opposite the applied horizontal temperature gradient, which is the positive x-direction, i.e. parallel to the axis of the roll. At the onset of convection, the diameter of the roll, $d_c = \pi / l_c$, is generally a decreasing function of R_h and Q_v. In all the cases treated, it holds that $d_c \lesssim 1$.

In an analysis of two-dimensional absolute and convective instabilities at the onset of convection in the model, Brevdo & Ruderman (2009*a*,*b*) pointed out that two-dimensional longitudinal wavepackets are absolutely unstable, for all the values of R_h and Q_v, because all the two-dimensional longitudinal normal modes are non-oscillatory. This observation is in contrast with the results of the present paper that on the one hand show that in the three-dimensional dynamics as in the two-dimensional one, the longitudinal mode is favourable, but on the other hand reveal that at the onset of convection the three-dimensional growing localized perturbations having locally the form of non-oscillatory longitudinal rolls can be either absolutely or convectively unstable depending on whether $R_h Q_v = 0$ or not.

From the results of table 3 we see that in all the cases the group velocity vector of the emerging marginally unstable three-dimensional wavepacket has zero y-component. This is well in accordance with the fact that the longitudinal modes, i.e. the x-independent two-dimensional modes, are favourable for the onset of three-dimensional convection. In a two-dimensional treatment of the longitudinal perturbations, the emerging wavepacket is absolutely unstable for all the values of R_h and Q_v considered; i.e. it has zero group velocity, which in such a treatment is the velocity in the y-direction. In a three-dimensional analysis, the convective instability at the onset of convection found to exist when $R_h Q_v \neq 0$ is due entirely to the three-dimensional effect. Specifically, since in the destabilization in the three-dimensional case the longitudinal modes are favoured, an added third dimension in a three-dimensional treatment compared with a two-dimensional treatment of longitudinal perturbations, i.e. the direction x added to the directions y and z in the analysis of wavepackets, does not change the component of the group velocity in the y-direction of the wavepacket, leaving it equal to the group velocity of a two-dimensional longitudinal mode, that is to say equal to zero. However, the component of the group velocity in the added

x-direction is not zero when $R_h Q_v \neq 0$, meaning absolute stability but convective instability at the onset of convection.

An absolute–convective instability dichotomy in a set of exact analytic solutions of the equations of motion in the model was discovered by Brevdo & Ruderman (2009*a*,*b*) for two-dimensional transverse disturbances. The dichotomy found in that two-dimensional analysis as well as the one in the present three-dimensional treatment can hopefully be used to explore experimentally and in a numerical nonlinear study the implications of two essentially different forms of linear destabilization, absolute and convective, for the emergence of fully developed nonlinear regimes. Such explorations can be facilitated by the fact that the dichotomies were found to exist in a set of exact analytic solutions of the equations of motion in a relatively simple model.

REFERENCES

Bahloul, A., Boutana, N. & Vasseur, P. 2003 Double-diffusive and Soret-induced convection in a shallow horizontal porous layer. *J. Fluid Mech* **491**, 325–352.

Bear, J. 1988 *Dynamics of Fluids in Porous Media*. Dover.

Brevdo, L. 1991 Three-dimensional absolute and convective instabilities, and spatially amplifying waves in parallel shear flows. *Z. Angew. Math. Phys.* **42**, 911–942.

Brevdo, L. & Ruderman, M. S. 2009*a* On the convection in a porous medium with inclined temperature gradient and vertical throughflow. Part I. Normal modes. *Transp. Porous Media.* **80**, 137–151.

Brevdo, L. & Ruderman, M. S. 2009*b* On the convection in a porous medium with inclined temperature gradient and vertical throughflow. Part II. Absolute and convective instabilities, and spatially amplifying waves. *Transp. Porous Med.* **80**, 153–172.

Briggs, R. J. 1964 *Electron-Stream Interaction with Plasmas.* MIT Press.

Delache, A. & Ouarzazi, M. N. 2008 Weakly nonlinear interaction of mixed convection patterns in porous media heated from below. *Intl J. Therm. Sci.* **47**, 709–722.

Delache, A., Ouarzazi, M. N. & Combarnous, M. 2007 Spatio-temporal stability analysis of mixed convection flows in porous media heated from below: comparison with experiments. *Intl J. Heat Mass Transfer* **50**, 1485–1499.

Drazin, P. G. & Reid, W. H. 1981 *Hydrodynamic Stability*. Cambridge University Press.

Gaster, M. 1968 The development of three-dimensional wave packets in a boundary layer. *J. Fluid Mech.* **64**, 654–665.

Gaster, M. 1975 A theoretical model of a wave packet in the boundary layer on a flat plate. *Proc. R. Soc. Lond.* A **347**, 271–289.

Gaster, M. & Grant, I. 1975 A theoretical model of a wave packet in the boundary layer on a flat plate. *Proc. R. Soc. Lond.* A **347**, 253–269.

Landau, L. D. & Lifshitz, E. M. 1959 *Fluid Mechanics*. Pergamon.

Narayana, P. A. L., Murthy, P. V. S. N & Gorla, R. S. R. 2008 Soret-driven thermo-solutal convection induced by inclined thermal and solutal gradients in a shallow horizontal layer of a porous medium. *J. Fluid Mech* **612**, 1–19.

Nield, D. A. 1990 Convection in a porous medium with inclined temperature gradient and horizontal mass flow. In *Heat Transfer 1990: Proceedings of the Ninth International Heat Transfer Conference, Jerusalem* (ed. G. Hetsroni), vol. 5, pp. 153–158. Hemisphere.

Nield, D. A. 1991 Convection in a porous medium with inclined temperature gradient. *Intl J. Heat Mass Transfer* **34**, 87–92.

Nield, D. A. 1994 Convection in a porous medium with inclined temperature gradient: additional results. *Intl J. Heat Mass Transfer* **37**, 3021–3025.

Nield, D. A. 1998 Convection in a porous medium with inclined temperature gradient and vertical throughflow. *Intl J. Heat Mass Transfer* **41**, 241–243.

Nield, D. A. & Bejan, A. 2006 *Convection in Porous Media*. Springer.

Nield, D. A., Manole, D. M. & Lage, J. L. 1993 Convection induced by inclined thermal and solutal gradients in a shallow horizontal layer of a porous medium. *J. Fluid Mech* **257**, 559–584.

Ouarzazi, M. N., Mejni, F., Delache, A. & Labrosse, G. 2008 Nonlinear global modes in inhomogeneous mixed convection flows in porous media. *J. Fluid Mech* **595**, 367–377.

Persson, A. O. 2006 Hadley's principle: understanding and misunderstanding the trade winds. *History Meteorol.* **3**, 17–42.

Qiao, Z. & Kaloni, P. N. 1997 Convection in a porous medium induced by an inclined temperature gradient with mass flow. *Trans ASME J. Heat Transfer* **119**, 366–370.

Straughan, B. 2004*a* Resonant penetrative convection. *Proc. R. Soc. Lond.* A **260**, 2913–2927.

Straughan, B. 2004*b* The energy method, stability and nonlinear convection. Springer.

Straughan, B. & Walker, D. W. 1996 Two very accurate and efficient methods for computing eigenvalues and eigenfunctions in porous convection problems. *J. Comput. Phys.* **127**, 128–141.

Twiss, R. Q. 1951 On oscillations in electron streams. *Proc. Phys. Soc. Lond.* B **64**, 654–665.

Weber, J. E. 1974 Convection in a porous medium with horizontal and vertical temperature gradients. *Intl J. Heat Mass Transfer* **17**, 241–248.